Optical Zener-Bloch oscillations in binary waveguide arrays

S. Longhi

Dipartimento di Fisica and Istituto di Fotonica e Nanotecnologie del CNR Politecnico di Milano, Piazza L. da Vinci, 32 I-20133 Milano (Italy)

PACS. 42.82.Et – Waveguides, couplers, and arrays .
PACS. 42.65.Sf – Dynamics of nonlinear optical systems; optical instabilities, optical chaos and complexity, and optical spatio-temporal dynamics .

Abstract. – Zener tunneling in a binary array of coupled optical waveguides with transverse index gradient is shown to produce a sequence of regular or irregular beam splitting and beam recombination events superimposed to Bloch oscillations. These periodic or aperiodic Zener-Bloch oscillations provide a clear and visualizable signature in an optical system of coherent multiband dynamics encountered in solid-state or matter-wave systems.

Light propagation in waveguide arrays has provided in the past few years a conceptually and experimentally relevant model to study the optical analogue [1–8] of Bloch oscillations (BO) and related effects typically encountered in solid-state or matter-wave systems [9, 10]. One of the major advantages offered by waveguide arrays as compared to other optical systems [11] is the possibility to easily perform a direct visualization of the wave packet dynamics in coordinate space [6] which is complementary to most usual frequency-domain (spectral) measurements [9, 11]. Recent experiments in waveguide arrays [6, 8] have reported the beautiful observation of optical Zener tunneling (ZT), thus motivating the study of multiband dynamics in these systems. In presence of a constant field, which yields a BO motion within a single band approximation, ZT usually manifests as a cascading of transitions to higher-order bands which results in the damping of the oscillatory BO motion or -in the spectral domain- in the broadening of the Wannier-Stark (WS) resonances [9,12]. In Ref. [6] a direct visualization of decaying BO via ZT to higher-order bands has been reported in a polymer waveguide array with a low refractive index contrast, which is analogous to BO decay observed in Bose-Einstein condensates in shallow lattices [10]. In the experiment of Ref. [6], the BO motion of a light wave packet in the first band of the array is periodically damped owing to the appearance of ZT which manifests itself as regular outbursts of radiation escaping at the turning points of the motion where the wave packet reaches the edge of the Brillouin zone in the reciprocal space. This decay of BO via periodic ZT bursts is irreversible and involves a cascading of transitions to higher-order bands. However, as discussed in the context of semiconductor superlattices [13, 14], a coherent dynamics instead of an irreversible decay process is expected when only two bands, coupled by ZT, are involved. In this case the dynamics of occupation probabilities in the two bands shows a complex coherent behavior which is related to the

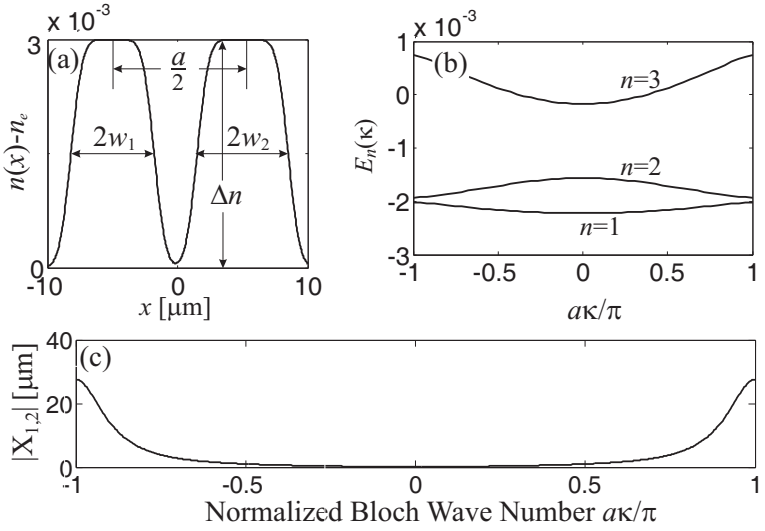

Fig. 1 – (a) Effective refractive index modulation (unit cell) of the binary array used in the numerical simulations. Parameter values are: $a = 20$ μm, $w_1 = 3.2$ μm, $w_2 = 3.5$ μm, $\Delta n = 0.003$, $\lambda = 1.44$ μm, $n_e \simeq 2.138$ (note that $w_1 \neq w_2$). (b) Band diagram for $F = 0$. n is the band index. The other parameter values are the same as in Fig.1(a). (c) Behavior of interband coupling coefficient $|X_{1,2}|$

spacing of the two interleaved WS ladders [14] and may even lead, under special conditions, to suppression of ZT.

In this Letter BO dynamics in a binary array of coupled optical waveguides is theoretically analyzed and shown to provide an ideal optical system for a direct observation of two-band coherent Zener-Bloch dynamics, in which ZT manifests itself as an aperiodic or periodic splitting and recombination of propagating light beam superimposed to the BO motion. The binary array [15] consists of a sequence of alternating single-mode optical waveguides of different widths $2w_1$ and $2w_2$, separated by $a/2$, showing the same refractive index peak change Δn [Fig.1(a)]. We describe light propagation in the array by a rather standard two-dimensional scalar Schrödinger-like equation [16,17], extended to include a transverse index gradient which simulates either transverse thermal heating of waveguides [6] or waveguide curvature [4,5]. By writing the electric field as $E(x, z, t) = \psi(x, z) \exp(ikn_e z - i\omega t) + c.c.$, where ω is the angular frequency of the field, $k = \omega/c_0$ its wave number in vacuum, and n_e an effective index of the structure [17], the evolution of the field envelope ψ along the propagation z direction satisfies the paraxial wave equation

$$i\hbar \frac{\partial \psi}{\partial z} = -\frac{\hbar^2}{2n_e} \frac{\partial^2 \psi}{\partial x^2} + [n_e - n(x)]\psi - Fx\psi, \tag{1}$$

where $n(x) - n_e$ is the effective modulation of the optical refractive index [17] in the transverse x direction [with $|n(x) - n_e| \ll n_e$], $\hbar = \lambda/(2\pi) = 1/k$ is the reduced wavelength, and F is the index gradient coefficient. For circularly-curved waveguides, F is related to the bending radius of curvature R by the simple relation $F = n_e/R$ [18]. Since the unit cell of the array is a dimer and supports two modes (namely the symmetric and anti-symmetric combinations of the modes guided by the narrow and wide waveguides), the band structure shows two

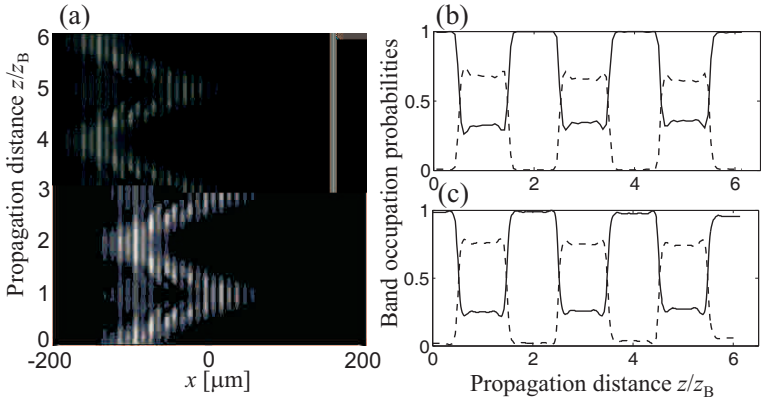

Fig. 2 – (a) Gray-scale plot showing beam intensity propagation in a 8-cm long binary array for $F = 5.52$ m^{-1}, corresponding to a Bloch period $z_B = 13.04$ mm. The input field is a Gaussian beam $\psi(x,0) = \exp[-(x+x_0)^2/w_0^2]$ with $w_0 = 45$ μm and $x_0 = 100$ μm. The geometrical parameters of the binary array are the same as those of Fig.1. (b) Numerically-computed evolution of band occupation probabilities P_1 and P_2 versus propagation distance. (c) Behavior of P_1 and P_2 as predicted by the two-level equations (3) and (4).

lowest-order bands [15], separated by a gap E_g which vanishes for $w_1 = w_2$. If the gap is large enough, i.e. if w_1 is sufficiently different from w_2 and the index change Δn is not too small, LZ is usually negligible at low or moderate values of F and BO occurs with a spatial period $z_B = 2\pi\hbar/(Fa) = \lambda/(Fa)$ (see, for instance, [4, 6, 21]). However, for $w_1 \simeq w_2$, the two bands are separated by a small gap and ZT is no more negligible, although it may be still disregarded for higher-order bands. A typical band diagram of the binary array [19] for $F = 0$ and $w_1 \simeq w_2$ is depicted in Fig.1(b) for parameter values typical of Lithium-Niobate waveguide arrays [20]. To study the role of ZT on BO dynamics, we numerically simulated propagation of a broad Gaussian beam for different values of the refractive index gradient F, i.e. of the Bloch period z_B. For the sake of simplicity, normal incidence has been assumed, so that at the input plane of the array the first band ($n = 1$) is mostly excited [16]. For very small values of F, a characteristic BO motion with period z_B is observed, however as F is increased, i.e. as z_B decreases, a sequence of beam splitting and beam recombination at planes $z = z_B/2, 3z_B/2, 5z_B/2, ...$ is observed, which is related to ZT as discussed below. The sequence is usually irregular, i.e. aperiodic, however at some special values of F it shows a nearly-periodic pattern. Since this ZT sequence is superimposed to a BO motion with period z_B, the resulting beam motion can be referred to as optical Zener-Bloch oscillations (ZBO). As an example, Figs.2(a) and 3(a) show typical numerical results demonstrating either nearly-periodic or aperiodic ZBO. In both cases the array length is 8 cm. Note that, for a curved waveguide array the values of index gradient F used in the simulations of Figs.2(a) and 3(a) correspond to a radius of curvature $R \simeq 38.7$ cm and $R \simeq 44.5$ cm, respectively. To relate the observed dynamics with ZT, we adopt a rather general technique developed in solid-state physics [12] and expand the wavepacket $\psi(x,z)$ as a superposition of Bloch states $\varphi_n(x,\kappa) = u_n(x,\kappa)\exp(i\kappa x)$ of the array, i.e. we set $\psi(x,z) = \sum_n \int_{-\pi/a}^{\pi/a} d\kappa c_n(z,\kappa)\varphi_n(x,\kappa)$, where n is the band index, $-\pi/a < \kappa < \pi/a$, $u_n(x+a,\kappa) = u_n(x,\kappa)$, and the normalization condition $\int_{-\infty}^{\infty} dx\varphi_{n'}^*(x,\kappa')\varphi_n(x,\kappa) \equiv \langle\varphi_{n'}(x,\kappa')|\varphi_n(x,\kappa)\rangle = \delta_{n,n'}\delta(\kappa-\kappa')$ holds. The occupation probability of band n is given by $P_n(z) = \int d\kappa|c_n(z,\kappa)|^2$.

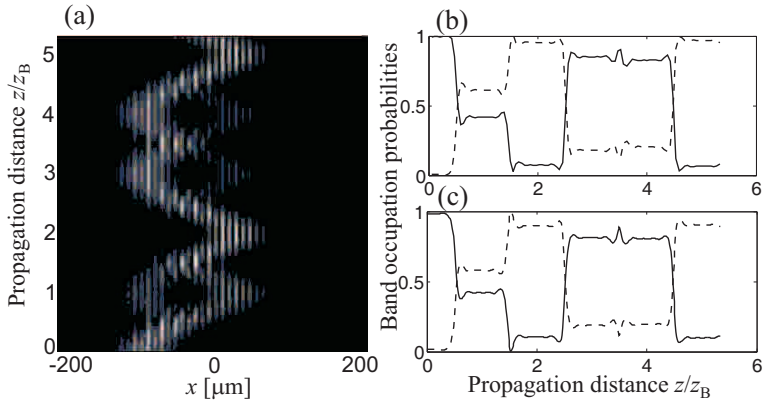

Fig. 3 – Same as Fig.2, but for $F = 4.8$ m^{-1} ($z_B = 15$ mm), corresponding to aperiodic ZBO.

For the binary array with the band diagram shown in Fig.1(b) and for near normal beam incidence, the main dynamics comprises only the two bands $n = 1, 2$. Figures 2(b) and 3(b) show the numerically-computed occupation probabilities for the two lowest-order bands versus propagation distance, corresponding to the spatial ZBO motion of Figs.2(a) and 3(a). Note that ZT is characterized by sharp and consistent interband transitions at planes $z = z_B/2, 3z_B/2, 5z_B/2, ...$ connected by plateau regions where ZT is small. In these connecting regions, the motion of the two wavepackets constructed by the superposition of Bloch modes belonging to the two lowest-order bands are independent each other and shows BO. Beam splitting and recombination is thus due to abrupt power transfer between the two wavepackets, which in the plateau regions move into opposite directions according to the semiclassical motion of a Bloch particle. To get deeper insights into the ZBO dynamics and to explain the existence of special values of F leading to a periodic motion, we consider the evolution equations for the spectral coefficients $c_n(z, \kappa)$, which read [12]:

$$i\hbar \frac{\partial c_n}{\partial z} = E_n(\kappa) c_n(z, \kappa) - iF \frac{\partial c_n}{\partial \kappa} - F \sum_l X_{n,l} c_l(z, \kappa), \tag{2}$$

where $X_{n,l}(\kappa) = X_{l,n}(\kappa)^* = (2\pi i/a) \int_0^a dx\ u_n^* (\partial u_l/\partial \kappa)$ and $n, l = 1, 2$ in the two-band approximation. The coupling term $X_{1,2}$ in Eq.(2) accounts for interband transitions, i.e. ZT. For a symmetric index profile $[n(x) = n(-x)]$, the Bloch functions $u_n(x, \kappa)$ can be taken such that $X_{1,1} = X_{2,2} = 0$ and $X_{1,2}(\kappa) = i\Theta(\kappa)$, with Θ real valued and $\Theta(-\kappa) = \Theta(\kappa)$. The numerically-computed behavior of $X_{1,2}$ for the binary array of Fig.1(a) is shown in Fig.1(c). For broad beam excitation at normal incidence, the values of coefficients $c_{1,2}$ at the input plane $z = 0$ are approximately given by $c_1(0, \kappa) \simeq g(\kappa)$ and $c_2(0, \kappa) \simeq 0$, where the spectrum $g(\kappa)$ is narrow around $\kappa = 0$. In this case, according to the acceleration theorem a solution to Eqs.(2) is simply given by $c_{1,2}(z, \kappa) = f_{1,2}(Fz/\hbar) g(\kappa - Fz/\hbar)$, where $f_{1,2}(\kappa)$ satisfy the two-level equations with periodic coefficients

$$iF \frac{df_1}{d\kappa} = E_1(\kappa) f_1 - iF\Theta(\kappa) f_2 \tag{3}$$

$$iF \frac{df_2}{d\kappa} = E_2(\kappa) f_2 + iF\Theta(\kappa) f_1 \tag{4}$$

with $f_1(0) \simeq 1$ and $f_2(0) \simeq 0$. The occupation probabilities of the two bands are then given by $P_1(z) = |f_1|^2$ and $P_2(z) = |f_2|^2$. ZT corresponds to non-adiabatic transitions at the points

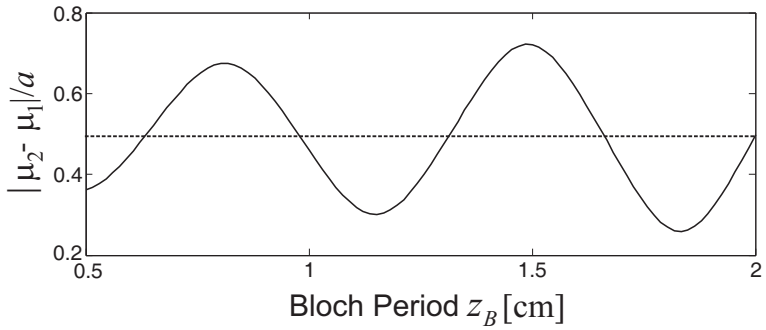

Fig. 4 – Behavior of normalized Floquet exponent difference $|\mu_2 - \mu_1|/a$ versus Bloch period z_B. The dotted curve corresponds to periodic ZBO with period $2z_B$.

of avoided crossing between the two bands, i.e at $\kappa = \pi/a, 3\pi/a, 5\pi/a, ...$, where the interband coupling Θ is largest and the energy separation $E_2(\kappa) - E_1(\kappa)$ smallest. This explains the characteristic dynamics shown in Figs.2(b) and 3(b), which is rather well reproduced by a numerical analysis of the two-level equations [see Figs.2(c) and 3(c)]. In order to explain the existence of periodic ZBO at special values of index gradient F, let us note that, according to Floquet theory the solution to Eqs.(3) and (4) is generally not periodic but characterized by the two periods $2\pi/a$ and $2\pi/|\mu_2 - \mu_1|$, where $i\mu_{1,2}(F)$ are the Floquet exponents of the system. However, for special values of F such that $|\mu_2(F) - \mu_1(F)|/a$ is a fractional number N/M (with N and M irreducible integers), the functions $P_{1,2}(z)$ are periodic with period Mz_B. For instance, for $|\mu_2 - \mu_1| = a/2$ the evolution of occupation probabilities is periodic with spatial period twice the Bloch period z_B. Figure 4 shows the numerically-computed behavior of $|\mu_2 - \mu_1|/a$ versus $z_B = \lambda/(Fa)$. Note that, at the intersections with the horizontal dashed line, ZBO are periodic with period $2z_B$, which is the case shown in Fig.2. The existence of periodic ZBO is closely related to the spectrum of Eq.(1), which for a two-band model is given by two interleaved Wannier ladders whose separation depends on the refractive index gradient F [14]. We can express the Wannier ladders for Eq.(1) in terms of the Floquet exponents $i\mu_{1,2}$ of the two-level equations (3) and (4) by extending the procedure of Ref. [12]. We look for solutions of Eqs.(2) in the form $c_n(z,\kappa) = \bar{c}_n(\kappa)\exp(-iEz/\hbar)$ and impose the periodic boundary conditions $\bar{c}_n(0) = \bar{c}_n(2\pi/a)$ to find the spectrum E. After some straightforward calculations, this yields for the spectrum the two interleaved Wannier ladders $E_n = -\mu_1(F)F + nFa$ and $E_m = -\mu_2(F)F + mFa$, where m and n are arbitrary integers and $i\mu_{1,2}$ are the Floquet exponents of the periodic system Eqs.(3) and (4). The condition for periodic ZBO is obtained when the spacing $F|\mu_2 - \mu_1|$ between the two ladders is a fractional multiple of the single ladder spacing Fa.

In conclusion, an optical realization of coherent BO motion superimposed to a periodic or aperiodic ZT sequence, leading to ZBO, has been proposed. This coherent dynamics should be directly visualized in a binary array with transverse refractive index gradient as a sequence of beam splitting and recombination.

Author E-mail address: longhi@fisi.polimi.it

REFERENCES

[1] Peschel U., Pertsch T., and Lederer F., *Opt. Lett.* , **23** (1998) 1701.

[2] Morandotti R., Peschel U., Aitchison J.S., Eisenberg H.S. and Silberberg Y., *Phys. Rev. Lett.*, **83** (1999) 4756.
[3] Pertsch T., Dannberg P., Elflein W., Bräuer A. and Lederer F., *Phys. Rev. Lett.*, **83** (1999) 4752.
[4] Lenz G., Talanina I. and de Sterke C.M., *Phys. Rev. Lett.*, **83** (1999) 963.
[5] Longhi S., *Opt. Lett.*, **30** (2005) 2137.
[6] Trompeter H., Pertsch T., Lederer F., Michaelis D., Streppel U., Bräuer A. and Peschel U., *Phys. Rev. Lett.*, **96** (2006) 023901.
[7] Trompeter H., Krolikowski W., Neshev D.N., Desyatnikov A.S., Sukhorukov A.A., Kivshar Yu. S., Pertsch T., Peschel U. and Lederer F., *Phys. Rev. Lett.*, **96** (2006) 053903.
[8] Fratalocchi A. and Assanto G., *Opt. Lett.*, **31** (2006) 1489.
[9] Glück M., Kolovsky A.R. and Korsch H. J., *Phys. Rep.*, **366** (2002) 103.
[10] Morsch O. and Oberthaler M., *Rev. Mod. Phys.*, **78** (2006) 179.
[11] Martijn de Sterke C., Bright J.N., Krug P.A. and Hammon T.E., *Phys. Rev. E*, **57** (1998) 2365. Sapienza R., Costantino P., Wiersma D., Ghulinyan M., Oton C.J. and Pavesi L., *Phys. Rev. Lett.*, **91** (2003) 263902. Ghulinyan M., Oton C.J., Gaburro Z., Pavesi L., Toninelli C. and Wiersma D.S., *Phys. Rev. Lett.*, **94** (2005) 127401.
[12] Callaway J., *Quantum Theory of the Solid State* (Academic Press, New York) 1974, p. 465-478.
[13] Rotvig J., Jauho A.P. and Smith H., *Phys. Rev. Lett.*, **74** (1995) 1831.
[14] Hone D.W. and Zhao X.-G., *Phys. Rev. B*, **53** (1996) 4834.
[15] Sukhorukov A.A. and Kivshar Y.S., *Opt. Lett.*, **27** (2002) 2112.
[16] Morandotti R., Mandelik D., Silberberg Y., Aitchison J.S., Sorel M., Christodoulides D.N., Sukhorukov A.A. and Kivshar Y.S., *Opt. Lett.*, **29** (2004) 2890.
[17] Sukhorukov A.A., Kivshar Y.S., Eisenberg H.S. and Silberberg Y., *IEEE J. Quant. Electron.*, **39** (2003) 31.
[18] For a curved waveguide with a local curvature $\ddot{x}_0$, in the paraxial approximation and after a Kramers-Henneberger transformation the curvature corresponds to a local index gradient $F = -n_e\ddot{x}_0$ (see, for instance, Eq.(2) of [5]). For circulary-curved waveguides, in the paraxial approximation one has $\ddot{x}_0 = \pm 1/R$, where R is the waveguide radius of curvature, and hence $F = \mp n_e/R$. See also Ref. [4].
[19] In Fig.1(b), $E_n(\kappa)$ is the eigenvalue of the Hamiltonian operator $\mathcal{H} = -(\hbar^2/2n_e)(\partial^2/\partial x^2)+V(x)$ with a potential $V(x) = n_e - n(x)$, where κ in the Bloch wave number, chosen in the first Brillouin zone, and n is the band index. Therefore, in the quantum context Fig.1(b) represents the energy band diagram of $\mathcal{H}$, and the energy $E_n(\kappa)$ thus increases with band index n. To understand the meaning of $E_n(\kappa)$ in the optical context, note that the effective propagation constant of the eigenmode (or supermode) of the array for the n-th band is given by $\beta_n(\kappa) = k[n_e - E_n(\kappa)]$, i.e. $n_e - E_n(\kappa)$ is the effective index of the supermode. A different way to denote the bands of the array, which was adopted in Ref. [16], is to plot the propagation constant $\beta_n(\kappa)$ instead of $E_n(\kappa) = n_e - \beta_n(\kappa)/k$. In this case $\beta_n(\kappa)$ decreases as the band index n is increased.
[20] Longhi S., Marangoni M., Lobino M., Ramponi R., Laporta P., Cianci E. and Foglietti V., *Phys. Rev. Lett.*, **96** (2006) 243901.
[21] Lenz G., Parker R., Wanke M.C. and Sterke C.M., *Opt. Commun.*, **218** (2003) 87.